Numerical investigation of crack self-sealing in cement-based composites with superabsorbent polymers

Rodríguez, C. Romero; Figueiredo, S. Chaves; Deprez, M.; Snoeck, D.; Schlangen, E.; Šavija, B.

DOI
10.1016/j.cemconcomp.2019.103395

Publication date
2019

Document Version
Final published version

Published in
Cement and Concrete Composites

Cement and Concrete Composites 104 (2019) 103395

Contents lists available at ScienceDirect

Cement and Concrete Composites

journal homepage: www.elsevier.com/locate/cemconcomp

Numerical investigation of crack self-sealing in cement-based composites with superabsorbent polymers

C. Romero Rodríguez[a,*], S. Chaves Figueiredo[a], M. Deprez[b], D. Snoeck[c], E. Schlangen[a], B. Šavija[a]

[a] Microlab, Department of 3MD, Faculty of Civil Engineering and Geosciences, Delft University of Technology, Stevinweg 1, 2628CN, Delft, the Netherlands
[b] PProGRess/UGCT, Geology Department, Faculty of Sciences, Ghent University, Krijgslaan 281 S8, B-9000, Ghent, Belgium
[c] Magnel Laboratory for Concrete Research, Department of Structural Engineering, Faculty of Engineering and Architecture, Ghent University, Tech Lane Ghent Science Park, Campus A, Technologiepark Zwijnaarde 60, B-9052, Ghent, Belgium

ARTICLE INFO

Keywords:
Superabsorbent polymers
Self-sealing
Cracks
Capillary absorption of water
Lattice model
Cement-based materials

ABSTRACT

Recently the concept of crack self-sealing has been investigated as a method to prevent degradation and/or loss of functionality of cracked concrete elements. To obtain self-sealing effect in the crack, water swelling admixtures such as superabsorbent polymers (SAP) are added into the cementitious mix. In order to design such self-sealing systems in an efficient way, a three-dimensional mesoscale numerical model is proposed to simulate capillary absorption of water in sound and cracked cement-based materials containing SAP. The numerical results yield the moisture content distribution in cracked and sound domain, as well as the absorption and swelling of SAP embedded in the matrix and in the crack. The performance of the model was validated by using experimental data from the literature, as well as experimentally-informed input parameters. The validated model was then used to investigate the role of SAP properties and dosage in cementitious mixtures, on the water penetration into the material from cracks. Furthermore different crack widths were considered in the simulations. The model shows good agreement with experimental results. From the numerical investigation guidelines are suggested for the design of the studied composites.

1. Introduction

The presence of a connected network of capillary pores in cementitious composites allows moisture to act as a carrier for aggressive species (i.e. chlorides, sulfates, CO_2, etc.)that may degrade the material. This process is further accelerated when cracking occurs. Cracks increase the surface area of the concrete element and therefore also the vulnerability of the material to the penetration of moisture and dissolved substances. As a consequence, corrosion of the reinforcement or expansive reactions might occur, generating further cracking within and further decreasing the durability of the element. To block water penetration into the matrix when cracks are present, superabsorbent polymers (SAP) have been proposed in literature to obtain a self-sealing effect in the crack [1]. In this context, self-sealing is referred as any reduction of the water flow in the cracks and consequently mitigated water penetration into the cementitious matrix.

SAP are three-dimensional network of crosslinked polyelectrolyte chains which can absorb large quantities of solution with respect to their own weight. The main pressures contributing to the swelling of SAP are of osmostic nature, due to both the elevated packing density of network strands and the difference in ionic concentration between the external solution and solution retained in the gel [2]. The pro-swelling forces in the gel are counteracted by the elastic deformation capacity of the polymeric chains and by acting external forces [3]. The polyelectrolyte gel reaches swelling equilibrium when pro-swelling and counteracting pressures are in equilibrium. The use of SAP as admixture in cementitious materials has been primarily investigated for the purpose of internal curing to minimize autogenous and drying shrinkage cracking [4] and for the generation of a uniformly distributed system of macropores to mitigate frost damage [5]. Other authors have also studied the influence of such polymers on the autogenous self-healing of concrete [6,7]. In this regard it has been suggested from experiments [7] that the water absorbed by the SAP in the crack is released later, causing dissolution of calcium-bearing phases and CO_2 and eventually the precipitation of calcite in the cracked space.

Requested SAP dosages in cement-based composites and properties of the SAP, such as swelling or absorption capacity and dimensions may differ for different applications. Typical dosages for internal curing purposes do not exceed 0.7 % by weight of cement [8,9], whereas for frost damage mitigation even lower quantities (about 0.3 %) are enough

* Corresponding author.
E-mail address: c.romerorodriguez@tudelft.nl (C.R. Rodríguez).

https://doi.org/10.1016/j.cemconcomp.2019.103395
Received 29 March 2019; Received in revised form 6 June 2019; Accepted 19 August 2019
Available online 22 August 2019
0958-9465/

[5,10,11]. In both cases the same studies present chosen average size of the swollen SAP in cement filtrate below 400 μm. For self-sealing and self-healing applications larger dosages of SAP are used, typically between 0.5 and 2. % by weight of cement, but varies for different types of SAP [7]. Sought dimensions at the swollen state in tap water are as large as possible for self-healing and self-sealing purposes [12,13].

Many experimental studies have been performed regarding hydrogel formation inside cracks in cementitious materials. In a work by Snoeck et al. [14] Neutron Imaging was performed during permeability tests in mortars with 1 % of SAP by weight of cement and using different types of SAP. The results presented in the study show slower depletions of the initial waterhead for mortars with SAP particles with respect to the plain reference mortar suggesting the desired self-sealing effect. Such mixtures had no additional water, therefore the differences in initial moisture content and transport properties of the mortar matrices might have influenced the results. Permeation tests performed by Hong and Choi [13] on SAP-containing mortars showed reductions of 75% and 63% of the water flow rates for crack widths of 250 and 350 μm, respectively, on mortars with 1% of SAP by weight of cement. In the former study, the swollen spherical SAP in the crack were observed by means of X-ray micro Computerized Tomography (μCT) and it was concluded that the majority of the particles filled only the macropore and portion of the crack within. In a work from Lee et al. [12] rather large dosages of SAP were used ($4-13\%$ by weight of cement) but the authors obtained cumulative flows well below 15 % of the reference ones for up to 300 μm cracks in cement paste, mortar and concrete. When observing through light microscopy the upstream surface of mortar samples subjected to permeability tests the authors could observe the hydrogel filling a significant portion of the visible crack. The authors also emphasized the need for limiting the initial swelling of SAP during mixing in order to obtain a larger sealing effect in the cracks.

Some analytical formulations have been proposed for the prediction of the self-sealing effect. In Ref. [15] the authors attempted to estimate the reduction of flow rates during permeation tests in mortar with spherical SAP. In the proposed formulation a fitting parameter was proposed to match modeled and experimental flow curves as the SAP dosage was increased in the material. Nevertheless, the authors could not assign a physical meaning to it and therefore, the use of the model remains limited to the type and percentages of SAP tested. Lee et al. [12] employed stereology to estimate the crack volume reduction due to SAP swelling as crack width and dosage, size and nominal swelling ratio of SAP are changed. Yet, the evaluated reduction could not be directly correlated to the water blocking effect.

Modelling-type experimentation could be advantageous for the optimization of self-sealing performance in cement-based materials with SAP while at the same time may offer insights into the mechanisms. However, it is of primary necessity that such models are representative of service life conditions and that input and output parameters are measurable and physically meaningful for all the composite phases. On the other hand, the aforementioned effect of SAP on promotion of self-healing of cracks in cement-based materials is strongly coupled with the short-term effect which is self-sealing. Therefore self-sealing models could be used as a basis for modelling mineral precipitation in cracks.

In this study, a numerical model is proposed to simulate capillary water absorption in unsaturated sound and cracked cementitious materials with SAP particles. The outputs of the model are the spatial moisture content distribution over time during capillary absorption experiments, as well as the amount of water absorbed by SAP and their swelling evolution. The Richards equation [16] is the governing equation which is coupled with the exponential equation describing the hydraulic diffusivity change with moisture content in building materials and with the water absorption kinetics law for SAP particles modeled as sink terms. A lattice-type approach was used for the spatial discretization of the domain. Heterogeneity of transport properties is explicitly modeled with this method, not only through the discrete distinction between SAP and mortar phases. The model was validated using experimental results and experimentally-informed input parameters available from literature or from experiments performed by the authors. A parametric investigation is then performed to study the influence of SAP absorption capacity and dosage in the mortar for different crack widths.

2. Formulation of the problem

In this section a brief derivation is offered of the governing equations for the studied problem. First, we introduce the simplified equations for the unsaturated flow in porous media and the empirical laws used for the derivation of its parameters in porous building materials. In the second part, the equation for the swelling kinetics of a single spherical SAP particle is reported.

2.1. Theory of unsaturated water transport in sound and cracked cement-based composites driven by capillary absorption

Starting from the two mass balance equations for air and water and Darcy's extended law for the flow velocity, one can arrive at the two-phase formulation of immiscible flow in homogeneous porous media. The resulting system can be simplified if certain conditions are met, leading to the Richards equation for the unsaturated water flow in porous media [16]. The conditions for the validity of Richards equation in cementitious materials have been reported in Ref. [17]. In sum, isothermal conditions around $20°C$ ensure the correctness of the assumption of uncoupling the water and air transport if they are assumed to be continuous throughout the pore space. Equation (1) reports the potential form of such equation:

$$C(\theta)\frac{\partial \varphi}{\partial t} = \nabla(K(\theta)\cdot\nabla\varphi) + S(\theta) \tag{1}$$

where φ is the hydraulic potential $[L]$, sum of the water head (q), capillary (ψ) and gravitational (z) potentials; $S(\theta)$ contains sinks or sources; $K(\theta)$ $[LT^{-1}]$ is the unsaturated permeability function and $C(\theta)$ $[L^{-1}]$ is the so-called capacity or storage coefficient described in Equation (2):

$$C(\theta) = \frac{d\Theta}{d\varphi} = (\Theta_s - \Theta_i)\frac{d\theta}{d\varphi} \tag{2}$$

where $(\Theta_s - \Theta_i)$ represents the difference between volumetric water content at saturation and at the start, which in a way represents the porosity accessible to water of the material, p $[-]$, and θ is the pores water saturation $[-]$.

If gravitational and waterhead potentials are considered to be negligible with respect to the capillary potential and the hydraulic diffusivity, $D(\theta)$ $[L^2T^{-1}]$, is defined as in Equation (3):

$$D(\theta) = \frac{K(\theta)}{C(\theta)} \tag{3}$$

Equation (1) can be transformed into:

$$\frac{\partial \theta}{\partial t} = \nabla(D(\theta)\cdot\nabla\theta) + s(\theta) \tag{4}$$

The advantage of the PDE formulated as in Equation (4) lies on the fact that $D(\theta)$ can be approximated, for the case of undamaged mortar, as [18]:

$$D(\theta) = D_0 e^{n\theta} \tag{5}$$

where n has been proven to lay between 6 and 8, varying little among materials [18]. In this work, n is assumed to have value 6. D_0 can be estimated from sorptivity experiments with good results, as proposed in Ref. [19] and shown in Eq (6):

$$D_0 = \frac{n^2 S_0^2}{(\Theta_s - \Theta_i)^2[e^n(2n-1) - n + 1]} \tag{6}$$

And the Sorptivity S_0 being defined as the slope of the best-fit line of the curve cumulative water absorption vs. $[T^{1/2}]$ for intially dried samples.

In the case of cracked mortar, the values of the hydraulic diffusivity in the cracked domain, $D_{cr}(\theta)$, are known to be much higher than those measured for the sound domain [20]. Using the definition of $D(\theta)$ and $C(\theta)$ given in Equations (3) and (2), respectively one can estimate the earlier as in the work of [21]:

$$D_{cr}(\theta) = -K_{cr} k_{cr}(\theta) \frac{dp_c}{d\theta} \tag{7}$$

In Equation (7) the crack relative permeability $k_{cr}(\theta)$ and the water retention curve $p_c(\theta)$ are assumed to follow Mualem [22] and van Genuchten [23] analytical formulations respectively, for certain values of the constants m and n calibrated for cracks by Ref. [21]. The saturated permeability of the cracked domain, K_{cr} is estimated by Poiseuille equation, assuming a laminar flow and a planar crack.

The system of equations describing the water absorption in unsaturated cement-based materials results then in the parallel implementation of Equation (4) and Equation (5) (or Equation (7) for the cracked domain).

For the problem of simulating capillary absorption of water in mortar the following boundary and initial conditions can be posed as in Eq (8):

$$\begin{aligned} &\theta = 1 && \text{on } \Gamma_1 \\ &\tfrac{\partial \theta}{\partial n} = 0 && \text{on } \Gamma_2 \\ &\theta(t=0) = \theta_0 && \text{in } \Omega \end{aligned} \tag{8}$$

Being Ω the entire domain and Γ_1 and Γ_2, two boundaries of Ω. θ_0 is the initial moisture content of the porous medium.

2.2. SAP water absorption and swelling kinetics

In Refs. [24,25] the swelling kinetics of spherical SAP particles are described as a diffusion-governed process depending only on their diameter, provided a certain ionic composition of the solution and a certain type of SAP. The model has been validated by monitoring the change of SAP's diameters in time [24]. The differently sized particles were immersed in a micro-bath and observed under an optical microscope. The author [24] assumed the hydrostatic pressure of the microbath negligible to the swelling pressure and a constant particle density to calculate the water uptake.

The swelling law proposed in Ref. [24] is presented in Equation (9) in terms of the swelling capacity at equilibrium of one individual SAP particle, $V_{SAP,max}$, and at any given time t, V_{SAP}.

$$\frac{dV_{SAP}}{dt} = k\left(V_{SAP,max} - V_{SAP}(t)\right) \tag{9}$$

The constant rate k, dependent on the particle diameter d_{SAP} , is shown in Equation (10).

$$k = r_1 d_{SAP}^{-r_2} \tag{10}$$

The constants r_1 $[L^{-r_2}/T]$ and r_2 $[-]$ depend on the swelling medium and the SAP type under consideration. Their values should be fitted from experiments carried out like in the work mentioned above while monitoring as well the amount of absorbed water.

Herein it is implicitly assumed that the volume of the particle at equilibrium, $V_{SAP_m,max}$, can be calculated as in Eq (11):

$$V_{SAP_m,max} = \frac{Ab_{sol}\rho_{dry}}{\rho_{sol}} V_{SAP,dry} \tag{11}$$

where Ab_{sol}, $[M_{sol}/M_{SAP}]$, is the absorption capacity of the SAP in the relevant solution, defined as the ratio between the weight of absorbed solution and the weight of dry polymer. Absorption capacity varies for the different solutions which the SAP may be subjected to Refs. [26,27]. ρ_{dry} and ρ_{sol} are the densities of the dry SAP and the solution, respectively and $V_{SAP,dry}$ is the volume of the dry irregular SAP particle.

3. Numerical and experimental methods

In this section we explain the numerical methods used to model the problem of water absorption in unsaturated mortar with distributed sinks. In addition, a description of the simulated experiments is offered, as well of the experimental input parameters used in the simulations.

3.1. Mesoscale lattice network model

Lattice network models have been successfully implemented to simulate mechanical behavior of cementitious materials [28]. Lately, they have also found applications in mass and ionic transport in such materials (i.e. moisture, water, chlorides) [21,29]. This type of models consists in an assembly of discrete two-nodes elements (lattice beams) that represents a continuum. For the modeling of transport, the lattice approach treats the transport as occurring along the beam elements in the lattice mesh. Other studies [30] defend the implementation of the transport in cracked materials occurring along the facets of the Voronoi poligons (in 2D). Herein, the transport is regarded as along the lattice beams.

For the discretization of the domain, the nodes are placed pseudo-randomly inside each cubic cell of a quadrangular grid. The specified sub-cell dimension with respect to the cubic cell determines the randomness of the set of nodes. For the mesh generation, we choose a randomness coefficient of 0.5. Subsequently, a Voronoi tessellation is performed with respect to the previously placed nodes in the domain. Nodes belonging to adjacent Voronoi cells are joined by lattice beams as schematized for a 2D geometry in Fig. 1.

The advantage of lattice-type models for unsaturated flow in cement-based materials is, among others, the explicit implementation of heterogeneities in the material. Sound cement paste, cracked domain, aggregates, SAP particles, Interfacial Transport Zone (ITZ) and other interfaces are assigned different lattice phases and corresponding transport properties. In this work the Anm model [31] was used for parking sand-shaped SAP into an initially empty prismatic container with non-periodic boundaries. The simulated SAP particles had the dimensions of the macropores left behind by SAP due to desorption during hardening of the mortar.

Next, a material overlay procedure is used: nodes in the lattice mesh

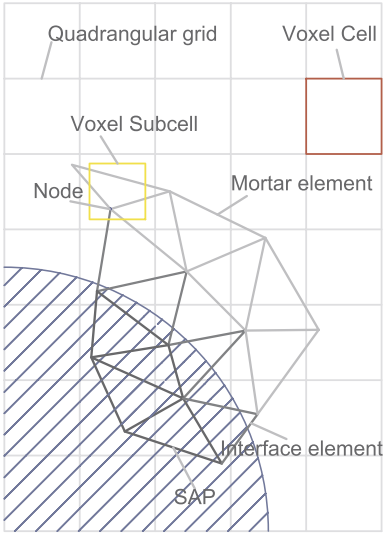

Fig. 1. Schematics of spatial discretization and mesostructure overlay procedure for the 2D case (modified from Ref. [29]).

are identified by overlapping them with the material mesostructure obtained with the Anm model (i.e. SAP and mortar phases). Similarly, beam elements with nodes belonging to the same phase are tagged as such, while elements bridging both phases are distinguished as interface elements. Schematics of the 2D procedure can be observed in Fig. 1. Although it has been widely reported that SAP enable internal curing in the cementitious matrix and that a higher degree of hydration is exhibited in the surroundings of the particle [9,32], we have not considered in the simulations heterogeneities in the transport properties of the mortar phase. SAP-mortar interface elements were assigned the same transport properties of the mortar.

3.1.1. Numerical implementation

If Equation (4) is discretized by using Galerkin method, in the context of lattice model its weak formulation in matrix form results as in Eq (12):

$$M\frac{\partial\theta}{\partial t} + K\theta = F \tag{12}$$

where the M and K are the mass and diffusivity matrices, respectively. F is the forcing vector, in which the Neumann-type boundary conditions and any sink/source terms are dumped. The elemental matrices and vectors described above are reported in Equations (13), (14) and (15)- for the ij element in its local reference system:

$$m_{ij} = \frac{A_{ij}l_{ij}}{6\omega}\begin{bmatrix} 2 & 1 \\ 1 & 2 \end{bmatrix} \tag{13}$$

$$k_{ij} = \frac{D_{ij}(\theta)A_{ij}}{l_{ij}}\begin{bmatrix} 1 & -1 \\ -1 & 1 \end{bmatrix} \tag{14}$$

$$f_{ij} = \begin{bmatrix} f_i \\ f_j \end{bmatrix} \tag{15}$$

A_{ij} and l_{ij} are the elemental area and length. While ω is a correction parameter for the volume of the single element. It has been proven that, being ω the ratio between the sum of all elements volume in the mesh and the volume enclosed by the mesh boundaries, its value results 3 for three-dimensional meshes [33].

Crank–Nicholson scheme is used for the time discretization as can bee seen in Eq (16).

$$\left(M + \frac{1}{2}\Delta t K^{n-1}\right)\theta^n = \left(M - \frac{1}{2}\Delta t K^{n-1}\right)\theta^{n-1} + \Delta t f \tag{16}$$

An iterative algorithm is avoided by calculating θ of the current time step (n) using the K matrix calculated at the previous step ($n-1$). Although an error is introduced in the solution of the system, it is small for appropriately short time steps. Such a procedure was used by Ref. [34] to model the drying of cementitious materials with good results.

3.1.2. Water absorption by superabsorbent polymers

On one hand, SAPs are regarded as sinks for the current physical problem. The volume of water absorbed by the node i belonging to the particle m at the current time step u was estimated as:

$$f^u_{i,SAP_m} = \frac{k_{SAP_m}(V_{m,max} - V^{u-1}_m)}{\sum_{i\in m} V_{cell,i}} V_{cell,i} \tag{17}$$

where $V_{cell,i}$ is the volume of the Voronoi cell associated to node i.

On the other hand, from the moment that SAPs are considered as another phase in the modeled mortar, transport properties need to be assigned to the beam elements corresponding to the SAP domain. The hydraulic diffusivity of SAP beam elements for the current time step was then estimated as:

$$D^u_{ij,SAP_m} = \frac{k_{SAP_m}(V_{m,max} - V^{u-1}_m)}{l_{ij}} \tag{18}$$

3.1.3. Self-sealing of cracks by SAP

The water - blocking effect of the individual SAP in the crack is considered in this model through three mechanisms. The hydraulic diffussivity of SAP elements decreases through Equation (18) as the SAP particle absorbs water and approaches its swelling equilibrium, eventually becoming an impermeable inclusion. At the same time, the crack width of SAP elements is reduced as the individual SAP swells and occupies more volume within the cracked macropore. Lastly, the former mechanisms are extended to other elements in the crack as the SAP swells beyond the macropore.

Procedurally, the swelling of SAP particles in the crack is actuated as follows. Firstly, the individual SAP swells to fill the macropore volume. When the cracked elements within the macropore are completely sealed the swelling beyond the macropore starts: an amount of cracked elements, contiguous to the individual SAP, are randomly tagged as such, which total volume corresponds to the volume of water absorbed at each time step. The new SAP elements are assigned transport properties corresponding to that specific SAP particle.

In implementing the aforementioned mechanisms, it was assumed that the single SAP particle grows from within every element of the macropore.

3.2. Experimental input parameters

In order to validate the use of the modified law of water absorption by SAP embedded in mortar (Equation (17)-(18)), experimental results described in Ref. [35] were used. The authors measured gravimetrically the capillary uptake of water in 28 days old sound mortars with SAP admixtures and in the corresponding reference plain mortars at different times during several days of absorption. The resulting absorptions for the first 6 h of the test were reported as sorptivity values for the studied mortars. Also the initial moisture content, θ_0, and the porosity accessible to water, p, were measured on the same specimens prior to the sorptivity test and after saturation, respectively. From these experiments, the mortars containing SAP type B were simulated because of the large availability of additional experimental data. In Table 1 the nomenclature used for the studied mixtures is summarized.

The same mortars containing water swelling admixtures and their references were reported to have closely similar capillary pore structures in Ref. [36]. Thus herein the sorptivity values obtained for the reference mortars were used to calculate the hydraulic diffusivity of the mortar matrix of corresponding SAP mortars. Nevertheless, it is largely known that the initial moisture content of porous materials influences the measured values of sorptivity. Many researchers proposed formulations to adjust measured sorptivity taking into consideration an initial uniform moisture content of the samples [37,38]. For low initial moisture saturations ($\theta_0 \leq 0.4$) the proposed formulations differ little, therefore in this work the simpler expression by Phillips [37] was employed (See Eq 19). Furthermore, the measured values of θ_0 were employed as initial conditions and the values of p were used for the calculation of the absolute water uptake obtained from the simulations. The input parameters used in the simulations, taken from Ref. [35], are summarized in Table 1.

$$S_0 = \frac{S}{(1-\theta_0)^{\frac{1}{2}}} \tag{19}$$

Table 1
Studied mortar mixtures, identifying SAP dosage m_{SAP}% (in mass of cement), total and effective water-to-cement ratios and transport properties.

Mixture	m_{SAP}%	w/c_{tot}	w/c_{eff}	$D_0\left[\frac{mm^2}{min}\right]$	p	θ_0
R0.50	0	0.50	0.50	0.0027	0.077	0.16
R0.41	0	0.41	0.41	0.0012	0.044	0.277
B1.0	1.0	0.50	0.41	0.00085	0.064	0.19

With respect to the superabsorbent polymers used in the experiments described in Ref. [35], their input parameters for the simulations were obtained from previous works [39,40]. The average largest dimension of SAP B particles at the dry state was reported to be $477 \pm 53\,\mu m$. The absorption capacity of the particles was $8.9\ g_{wat}/g_{SAP}$ during mixing of the mortar and the resulting macropores were sized $877 \pm 98\,\mu m$. In demineralized water the particles absorbed $283\ g_{wat}/g_{SAP}$. The particles density resulted $700\ kg/m^3$. In addition, the constants describing the swelling rate of SAP B in demineralized water were fitted as in Esteves [24] yielding the following formulation for the rate k where d_{SAP} is expressed in μm: $k = 112075\ d_{SAP}^{-1.828}$.

For the validation of the crack self–sealing model, the experimental results described in Ref. [14] were used. The authors used Neutron Imaging (NI) to monitor water transport in cracked B1.0 mortar specimens sized $100 \times 100 \times 28\ mm^3$. They correlated the self-sealing effect provided by SAP particles in the crack to the water penetration not only in the crack but specially into the mortar in perpendicular direction to the crack surfaces. Unfortunately, the input parameters were not available for the curing regime which the tested samples were subjected to. Nevertheless, in this work a fitting procedure was implemented to estimate the hydraulic diffusivity of R0.41 from the vertical moisture profiles obtained in Ref. [14] for B1.0 samples and the initial moisture content was assumed as 0.19 as measured from Refs. [35,41] for same B1.0 mortar and different curing regimes. A lattice with characteristic voxel size of 0.25 mm was used for the simulations. The mesh had dimensions of $25 \times 28 \times 3\ mm^3$, for a total of 134400 nodes and 955337 lattice elements. In Fig. 2 simulated moisture profiles over a period of 4 h and radiograph after 60 min of simulated absorption for a value of $D_0 = 0.006\ \frac{mm^2}{min}$ are shown and compared to the experimental results.

3.3. Experimental methods

MicroCT was performed at the Centre for X-Ray Tomography of Ghent University of crack self-sealing in mortar at equilibrium. This experiment was used to assess the extent of swelling of single SAP particles present in the crack.

The experimental setup HECTOR [42] consisted of a 240 kV X-ray tube from X-RAY WorX operated at $150\ kV$ and $74\ \mu A$. For each scan 2400 projection images were recorded using a PerkinElmer 1620 flat-panel detector. The Source-Detector-Distance was $1167\ mm$ and the Source-Object-Distance was $65\ mm$ resulting on a voxel size after reconstruction of $11\ \mu m$. The obtained images were reconstructed using the Tescan XRE reconstruction software Octopus Reconstruction © and

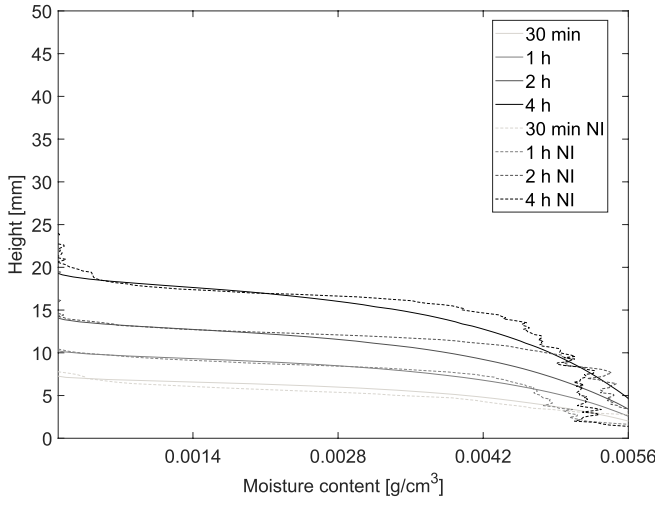

Fig. 2. Comparison of experimental and simulated results on capillary water absorption by B1.0 mortar with $D_0 = 0.006\ \frac{mm^2}{min}$: experimental and simulated vertical moisture profiles at 30, 60, 120 and 240 min.

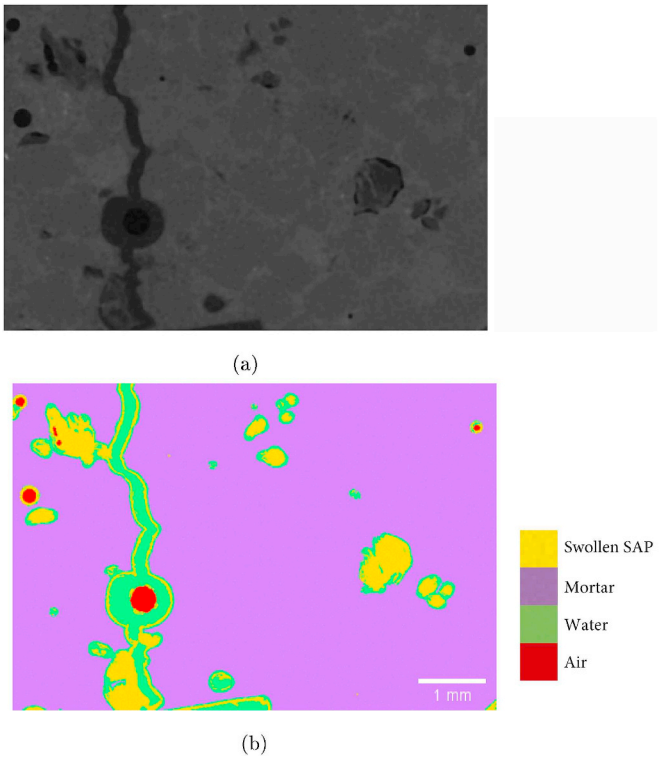

Fig. 3. Gray value image (a) and segmentation (b) of SAP in the crack and embedded in the matrix through Trainable Weka Segmentation plugin.

the data anlysis was performed with the open source software ImageJ.

The mortar mixture B1.0 was cast in grooved cylindrical moulds and cured until the age of 7 days at $21°C$ and 95 % of Relative Humidity. The cyclinders had a diameter of $16\ mm$, with two diametrically parallel prismatic grooves of $2\ mm$ side, and a height of $15\ mm$. At the age of 7 days the moist samples were wrapped with adhesive tape and split on a Brazilian Splitting configuration by means of a small compression/tension press. The two halves were kept together because of the wrapping in order to avoid loss of material during the splitting. Artifical crack widths of $200\ \mu m$ were generated within the groove of the split samples as follows. The two halves of the discs are fixed together by gluing them at the edges of the grooves. The desired crack width was steered by inserting prismatic bars with width equal to the groove width plus the desired crack width. The cracked cylinders were immersed in distilled water for another 3 days and later throughout the scan.

The swollen SAP particles in the crack were segmented using a Trainable Weka Segmentation (TWS) plugin [43] due to the similarity in Gray Values of water and swollen SAP in the crack. In Fig. 3 an example is shown of a swollen SAP in the crack from a resulting tomography and segmented by using TWS. The SAP macropores embedded in the sound matrix were segmented through simple thresholding operation. The volume of each macropore was estimated through 3D Object Counter and the probability density function of the volumes were estimated by fitting the volume data to a normal Kernel Density (KD) distribution. The obtained KD was used to generate 10000 samples with size equal to the number of segmented SAP particles in the crack. The total volume of macropores of each of the 10000 samples was used to calculate an average ratio between swollen SAP gel volume and macropore volume, equivalent to the ratio between swelling capacity of the SAP in the crack and that during mixing. Throughout this paper, we call this ratio swelling ratio, S_{cr}/S_{mix}. The resulting value, 1.37, was used as input for the model as per limiting the swelling of SAP type B in the crack.

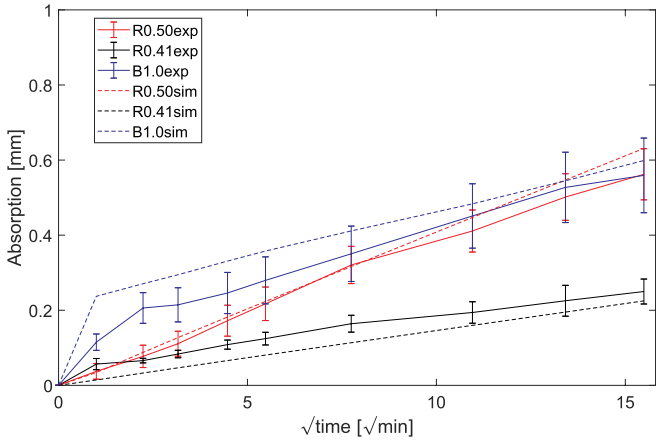

Fig. 4. Simulated and experimental capillary water uptake in mortars R0.50, R0.41 and B1.0.

4. Model validation

4.1. Capillary absorption of water in sound mortar

The capillary uptake of water by undamaged mortar with SAP admixtures, B1.0, was simulated in this section. Also the reference mortars R0.41 and R0.50 were simulated. The mesh had dimensions of $40 \times 10 \times 10\ mm^3$, for a total of 128000 nodes and 942877 lattice elements. In Fig. 4 a comparison is shown between experimental and simulated results of the mortars above. The simulated curve of B1.0 reports the average of three simulated mesostructures. The absorption I is normalized as in Eq (20):

$$Absorption(t) = \frac{m_{water}(t)}{A\rho_{water}} \tag{20}$$

where $m_{water}(t)$ is the uptaken mass of water at the time t, A is the area exposed to water and ρ_{water} is the density of water at $20°C$.

In general, the simulated water absorptions agree well with the experimental ones for the studied mixtures. Mortar R0.50, with the highest water-to-cement ratio and transport properties, presented the highest bulk water absorption. On the other hand the mortar containing SAP particles, B1.0, presented considerably higher values of absorption when compared to its reference mortar R0.41 despite the smaller values of D_0. In the simulations, this is due to the presence of distributed discrete SAP particles modeled as sinks which absorb water rapidly when reached by the water front. Similar results were also obtained experimentally by Ref. [44] because during capillary absorption the SAP (also present at the surface) quickly absorbs and retains the absorbed water, leading to a higher observed mass.

The absorption curve of B1.0 presented a marked nonlinear behaviour as in the experiments which deviates from the typical linear behavior found for plain mortars. This is attributed to the contrast in transport properties of mortar and SAP phases, especially at the start of the absorption when the value of D_0 is minimum for the mortar and maximum for the SAP.

In experiments, initial fast uptakes of water during sorptivity tests are commonly found in mortar with high macroposity at the surface subjected to saturation [18]. One could argue that the surplus in absorption of water is an effect of the presence of macropores rather than of the presence of embedded SAP. Nevertheless, in a work of [45] where the authors studied the effect of different levels of air entrainment in concrete on the sorptivity, no clear trend was found to correlate the percentage of air voids with the mild increases or decreases of the sorptivity with respect to the reference samples. Furthermore, specimens preconditioned in the oven at $50°C$, like in the results used for the validation, the sorptivity decreased for increasing percentages of air entrainment. Moreover these decreases were not greater than 10 % with respect to the reference sorptivity.

4.2. Self-sealing of cracks by superabsorbent polymers in mortar

Three mesostructures were used to simulate fracture in a Wedge Splitting Test (WST) configuration through lattice fracture model. The modeled mesostructures contained 1 % of SAP by weight of cement in the mortar, which results approximately in 5 % of SAP macropores by volume of simulated mortar specimen. Lattices with characteristic voxel size of 0.25 mm were used for the spatial discretization. The meshes had dimensions of $25 \times 28 \times 3\ mm^3$, for a total of 134400 nodes and 955337 lattice elements. Although the input parameters for the fracture model such as the actual micromechanical properties of the cement paste in the mortar, aggregates and interfacial transition zone were unknown, the authors assigned lower mechanical properties to elements corresponding to SAP macropores and interface phases than to the (hypothetically homogenoeus) mortar phase as suggested in Ref. [46]. In this way more realistic crack patterns were obtained for the capillary water absorption simulations (see Fig. 5). In literature, it is found that SAP act as crack initiator and are available upon liquid intrusion [47,48]. The resulting cracked elements were assigned crack widths of 200 μm as the ones measured at the tip by Snoeck et al. [14]. This implies a mismatch of 40 μm in internal crack width between experimental specimens at a crack depth of 16 mm and the simulated 16 mm-deep crack, for a cracked volume difference of 9 %. Thereafter the damaged lattice elements were assigned transport properties calculated following the formulation explained in Equation (7).

The horizontal water profiles measured through Neutron Imaging in three cracked mortar samples from mix design B1.0 were compared to the simulated results at 1, 5, 15, 30 and 60 min of capillary water absorption in Fig. 6. The experimental profiles were measured at heights not in correspondence of the reinforcement where the porosity of the material at the mortar-reinforcement interface may be different from the bulk matrix porosity. In the simulated profiles as well as in the NI profiles, the data points correspond to the moisture content averaged through the thickness of the mortar. Therefore localized anomalies on the horizontal water penetration due to the presence of superabsorbent polymers are smoothed and partially lost.

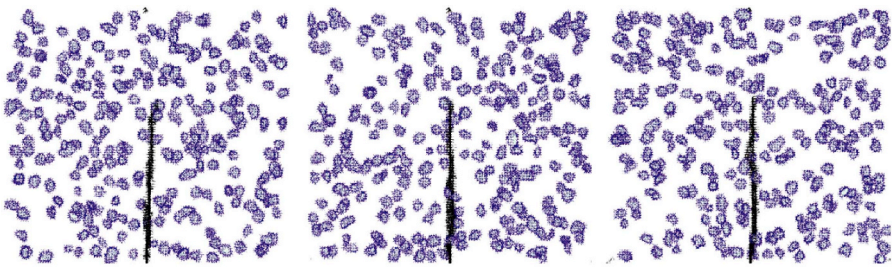

Fig. 5. Simulated mesostructures and crack patterns from WST simulations.

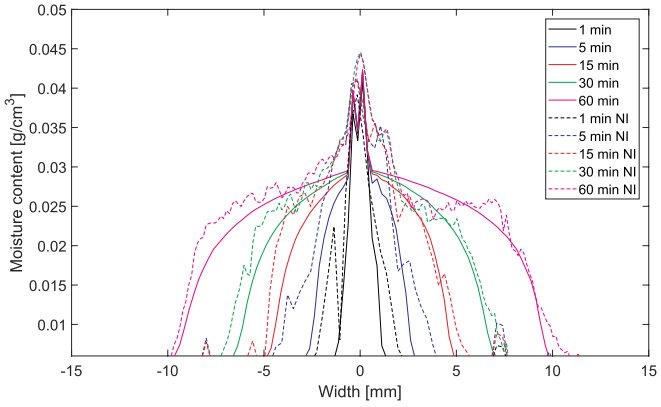

Fig. 6. Horizontal water profiles in B1.0 at 1, 5, 15, 30 and 60 min of capillary absorption of water, measured through NI and simulated.

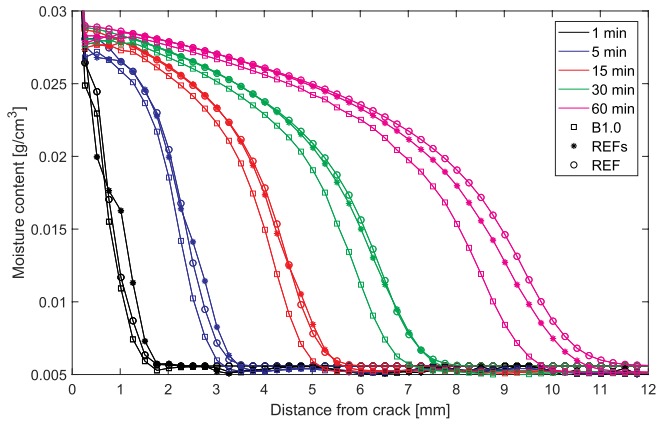

Fig. 7. Simulated horizontal moisture profiles of cracked mortar: without SAP (REF), with matrix-embedded SAP only (REFs) and with embedded and in-the-crack SAP (B1.0).

From the comparison between the profiles, there seems to be a very close agreement between experimental and simulated profiles. The penetration of the wetting front perpendicular to cracks as well as the moisture content distribution are captured well by the model. In the model the retardation of the water front penetration is due to swollen SAP in the cracks as well as those embedded in the matrix. To discriminate the role of hydrogel formation in the crack on the retardation of the water penetration perpendicular to cracks in Fig. 7 a comparison is reported of three simulated results in: cracked mortar without SAP (REF), cracked mortar with matrix-embedded SAP only (REFs) and cracked mortar with embedded and in-the-crack SAP (B1.0). The three of them are simulated with same input parameters D_0, p and θ_0 so that the transport in the cementitious matrix occurs in the same fashion.

Modest but tangible differences can be noticed in water penetration and moisture contents between B1.0 samples and the reference mortar with no admixtures (REF) since the beginning of the simulation, which are accentuated over time as seen at 60 min. The contribution of the embedded SAP on delaying the penetration of the water front is subtler and can be just observed after 60 min of capillary absorption of water for the matrix transport properties studied herein. For practical implications it can be considered negligible.

It can be observed from the results shown in Figs. 6 and 7 that the self-sealing performance of B1.0 was modest when compared to a reference plain mortar with same transport properties and initial conditions. The authors of this experimental study [14] noticed that their results were somehow different from their estimates which were obtained by assuming an absorption capacity of the SAP upon contact with tap water of 148.9 g_{wat}/g_{SAP} while in the simulations we use a value of 12.193 g_{wat}/g_{SAP}.

5. Parametric study of crack self-sealing and discussion

In this section, parameters such as absorption capacity of the superabsorbent polymers under constraint, their dosage in the cementitious material and the crack width are studied through simulations with the developed model. In all the simulations the transport properties of the mortar matrix are invariants, as well as their relative input parameters, with values as described in the previous section. The objective is to discuss the influence of these factors on crack self-sealing and to provide recommendations for the design of cement-based materials with SAP for self-sealing purposes.

5.1. Influence of SAP absorption capacity in the crack

When visualizing the swollen gel in the crack from different experimental studies it is obvious that the self-sealing effect provided by these polymers depends strongly on their absorption capacity under constraint. Lee and co-authors [12] found generous formation of hydrogel in the cracks coming from highly irregular SAP particles as observed through light microscopy while Hong and Choi [13] employed X-ray tomography to observe the swelling of spherical SAP particles and concluded that this was limited to the volume ascribed by the cracked macropore. Spherical SAP possess a high surface tension due to the polymerization technique through which they are produced (inversion polymerization). Irregular, bulk polymerized SAP, seem to be more flexible.

Furthermore, this swelling capacity fluctuates when subjected to wetting–drying cycles as demonstrated in a study by Lee et al. [27] where the authors explain the reduction of swelling capacity not only due to calcium ions binding in the polymeric chains but also the eventual recovery due to ion exchange in alkaline solutions. Hence, the influence of different levels of swelling capacity in the crack on the mechanism is also simulated in this section.

Fig. 8 shows the moisture contours and swollen gel in the crack in mortar for different absorption capacities of the SAP. In the model this is accounted for by setting a cuttoff to the maximum absorption of water and subsequent swelling by the particles.

The moisture contours show that the water penetration from the crack becomes slower as the amount of swollen gel increases. Furthermore, the distribution of the moisture content changes dramatically. The zones with higher degree of saturation 0.8–1.0 become narrower and correspondingly the zones with saturation levels between 0.6 and 0.8 become wider. This effect is probably related to the fact that as the swollen gel volume increases in the crack, bigger portions of the crack surfaces come into contact with gel and locally water penetration from those surfaces is slowed down. As a consequence, there exist gradients of moisture along the crack walls and not only perpendicular to them. As the swollen gel increases in volume the later effect becomes more severe in localized zones around the SAP (see Fig. 8d).

The re-swelling capacity of the SAP particles in the crack is not straight forward to be measured, especially when coupled with the absorption of water under pressure of the SAP. Some guidelines have been summarized in Ref. [26].

5.2. Influence of SAP dosage

Perhaps the most obvious way of increasing the likelihood of obtaining self-sealing effect is to increase the amount of SAP in the cementitious mixture. The presence of increasing evenly distributed macropores lead to stress concentrations around them and therefore to a higher chance of exposing more of these macropores along the crack path [46]. Nevertheless, at the levels of incorporation of SAP for the purpose of self-sealing, typically between 0.5 % and 1.0 % by weight of cement, decreases of the compressive strength in the order of 20 % to

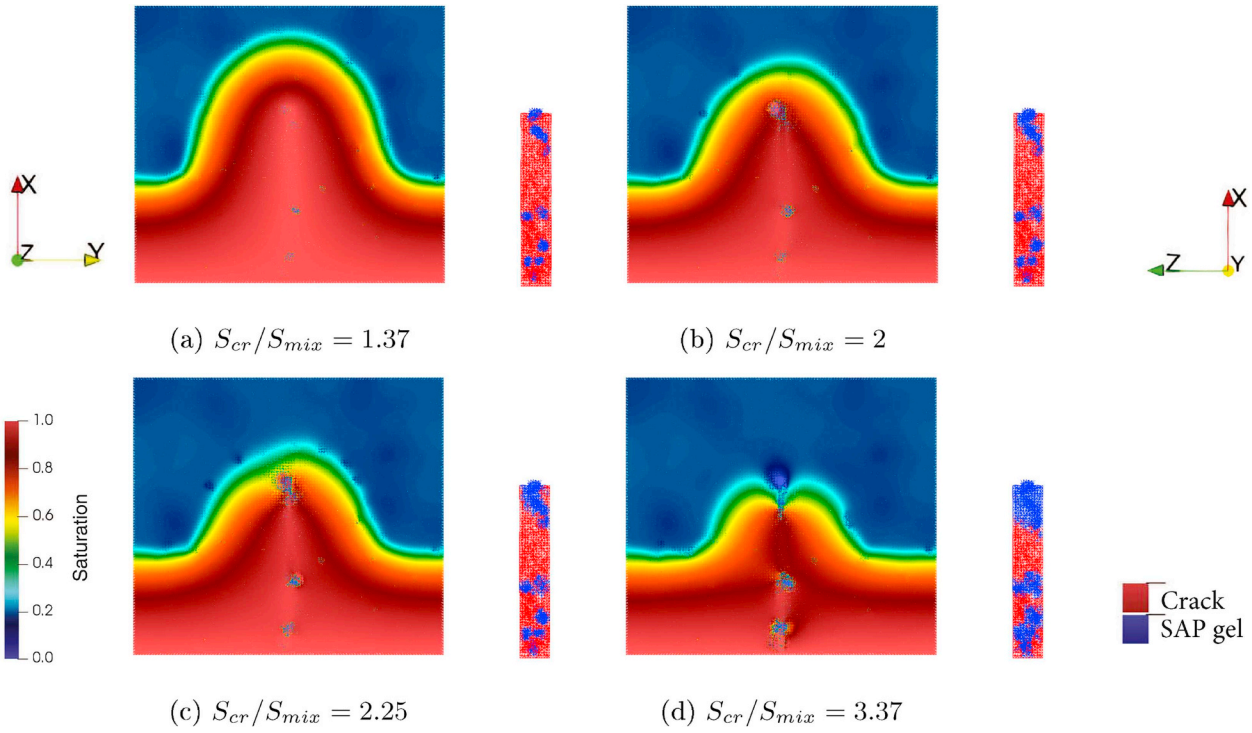

Fig. 8. Moisture contours and respective swollen gel in the crack after 60 min of water absorption in mortar with 1.0 % of SAP by weight of cement, crack width of 200 μm and different swelling ratios of the SAP in the crack: a) 1.37, b) 2, c) 2.25 and d) 3.37.

40 % are generally obtained in mixtures with relatively high water-to-cement ratio [13,39]. The latter effect is explained in literature as due to the role of SAP as crack initiator, demonstrated by the observed swelling of the particles when exposed to moisture uptake. The negative effects on the mechanical properties of the material are unwanted because on one hand we have a material with high crack self-sealing capacity whereas on the other hand it is more prone to crack formation.

In Fig. 9 a, b and c three simulated mesostructures of SAP mortar are shown with 0.5 %, 1.0 % and 1.5 % by weight of cement. The SAP particles were parked randomly with Anm model by using the same seed. Thereafter, fracture lattice simulations were performed to obtain the cracked meshes. Fig. 9d, e and 9f show the moisture contours after 60 min of capillary absorption simulations on these cracked meshes, whereas Fig. 9d, e and 9f show the cracked space of the respective mesostructures and the volume occupied by SAP gel. A fixed ratio between absorption capacity of the SAP in the crack and during mixing of 2.25 was used in the three simulations. Input parameters for the simulations were identical.

Noticeable differences can be observed by comparing the simulated results of mortars with different SAP dosages. The role of embedded SAP in the capillary absorption of water in the matrix can be studied from the vertical water penetration. In a study from Ref. [49], the authors noticed that for certain transport properties of the matrix, embedded SAP could actually behave as impervious inclusions after complete swelling in the macropore. Similar to how aggregates influence the transport of moisture in concrete [50], such inclusions might delay the wetting front penetration with respect to a reference mortar with same transport properties and no SAP. For increasing number of embedded SAP, this effect was expected to be accentuated. Notwhithstanding in the simulations, this effect accounts only for a small contribution on the retardation of the wetting front as well as for the water content distribution. This contribution is also present as the wetting front advances horizontally yet the influence of the transport in the crack is still present even when the dosage is kept constant as shown previously in Fig. 7.

The moisture contours show decreasing penetration depths of the water front for increasing dosages of SAP in the mortars and therefore higher amounts of SAP particles in the crack. This does not come as a surprise since it is expected that a higher volume of hydrogel forming in the crack contributes to decreasing the flow of water in the crack. Ideally, a plug of hydrogel would form at a certain height along the crack depth and completely stop the flow of water upwards. In the simulations shown in Fig. 9, this happens only for the mortar containing 1.5 % of SAP by weight of cement. In the other cases, although hydrogel is formed they form separate clusters which locally prevent the penetration of water into the matrix, while capillary rise of water in the crack still occurs.

As seen in the case of increasing swelling ratios of the SAP, here too the zones with saturation in the range 0.8–1 decrease in area for higher dosages of SAP in the simulated mortars.

5.3. Influence of crack width

The choice of SAP size, dosage and swelling and absorption capacity during mixing and in neutral to acidic solutions govern the crack-sealing capacity of the cementitious system. Yet, this sealing capacity will be limited as the crack widths under consideration are increased. It is important thus to evaluate how the self-sealing effect of SAP in the crack, in terms of water penetration into the cementitious matrix, changes with increasing crack widths.

Capillary absorption of water is again simulated for cracked mortar with SAP. Three different crack widths are used in the simulations: 200 μm, 300 μm and 500 μm. It is assumed that the transport properties of cracked elements is not affected by the crack width and just the proportion between cracked volume and swollen gel influences the variation in water permeation into the matrix. In Fig. 10 an example of such changes arising from the simulations results at $t = 60\ min$ are shown. The swelling in the crack to swelling during mixing ratio was 2.25 and the SAP dosage was 1.0 %. The aforementioned assumption would not be appropriate for crack widths above 500 μm since the capillary rise in the crack and thus the hydraulic diffusivity of the cracked elements would be certainly lower as shown in Ref. [51], which is not

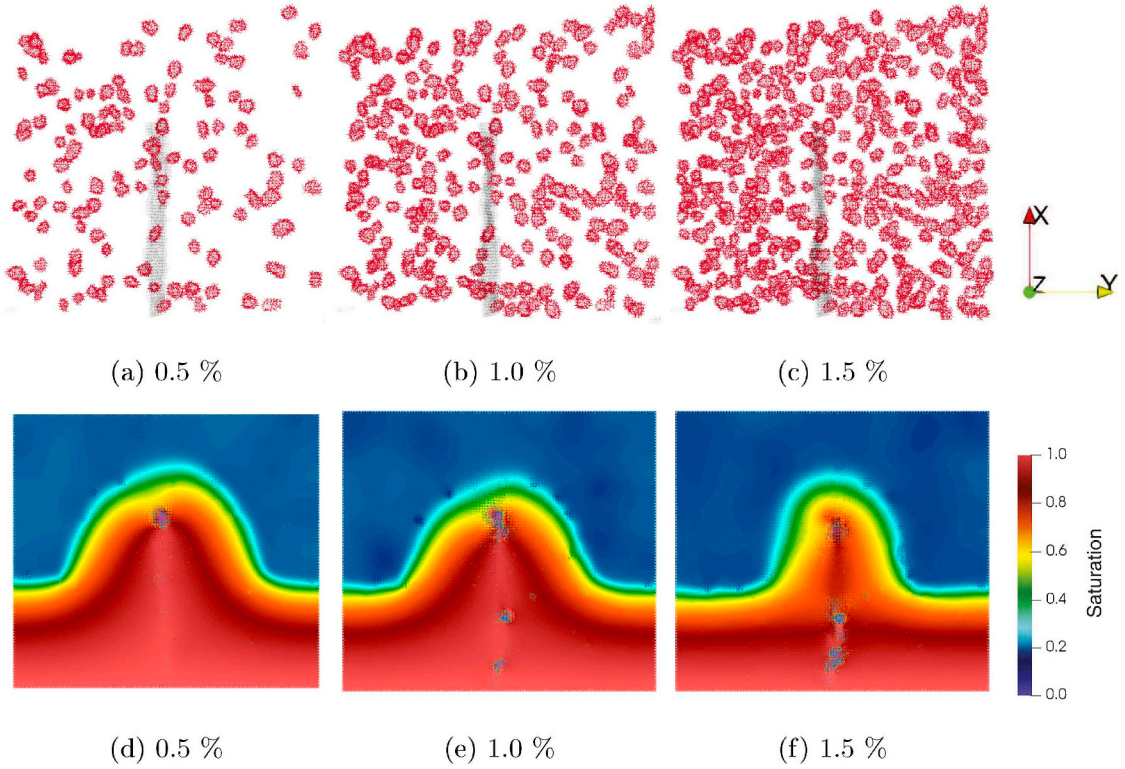

Fig. 9. Cracked mesostructures -a, b, c-, and moisture contours -d, e, f-of mortar with SAP in dosages 0.5 %, 1.0 % and 1.5 % by weight of cement, after 60 min of capillary water absorption. Crack width was kept as 200 μm and swelling ratio of 2.25.

accounted for in Equation (7).

As expected, the simulation results show that for wider cracks, there is less blockage of water in the crack and therefore water can penetrate more readily into the matrix. In particular, almost indistinguishable differences where found when the crack is wider than 300 μm for these specific material parameters. Also the anomalies in the moisture content distribution are gradually lost with an increase of the crack width.

5.4. Discussion

Fig. 11 reports the horizontal water penetration depth in cracked mortar with SAP normalized to the penetration depth of its reference without water swelling admixtures, h_{pen} (Eq 21), as a function of the chosen SAP dosage and ratio of swelling capacity in the crack to swelling capacity during mixing.

$$h_{pen} = \frac{d_{REF} - d_{SAP}}{d_{REF}} \tag{21}$$

According to the above definition h_{pen} valued 1 translates to a fully blocked crack water flow, while a value of 0 means that no difference is found between the reference mortar and the SAP mortar in terms of water front penetration. Therefore h_{pen} can be interpreted as a crack self-sealing efficiency. In the graphs in Fig. 11, h_{pen} is reported for different crack widths (200 μm -a-, 300 μm -b- and 500 μm -c-).

If we compare the surface plots corresponding to simulations with different crack widths some observations can be made. Whereas 100 % sealing can be obtained in mortar with crack width of 200 μm and for a dosage of 1.5 % SAP and swelling ratio of 3.37, as the crack width increases from 200 μm to 300 μm and 500 μm, the obtained healing promptly decreased to 50 % and 30 %, respectively for the same parameters. Likewise, fewer combinations of those parameters yield substantial reductions in water penetration as cracks widen. However in this parametric analysis the self-sealing capacity of mortar with SAP is underestimated for wedge-like cracks since the error computed in the calculation of cracked space volume increases for rising values of the crack tip as discussed in Section 4.2.

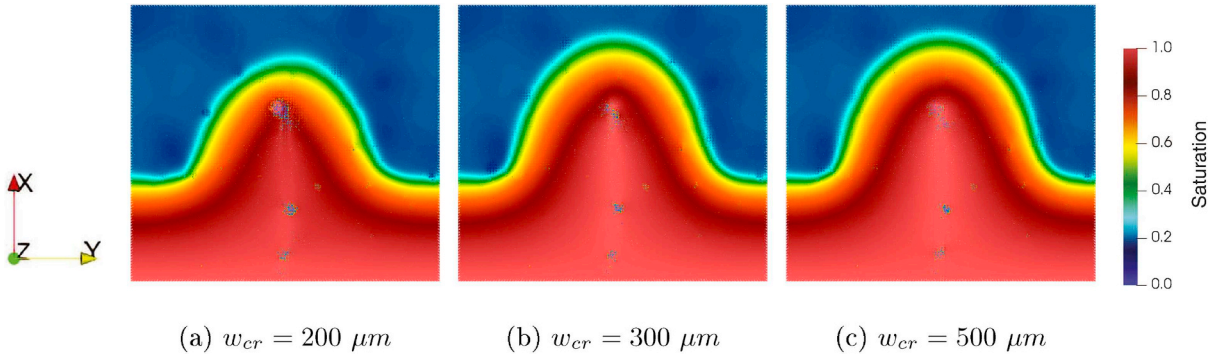

Fig. 10. Moisture contours of cracked mortar with SAP for different crack widths -a) 200 μm, b) 300 μm, c) 500 μm- after 60 min of capillary water absorption. Dosage and swelling ratio were kept constant as 1.0 % and 2.25, respectively.

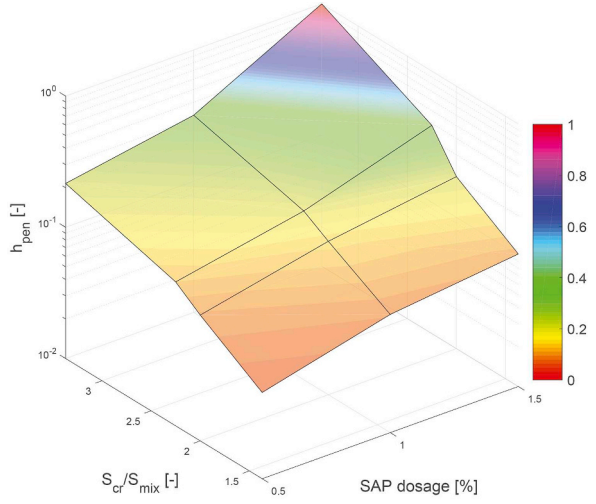

(a) $w_{cr} = 200\ \mu m$

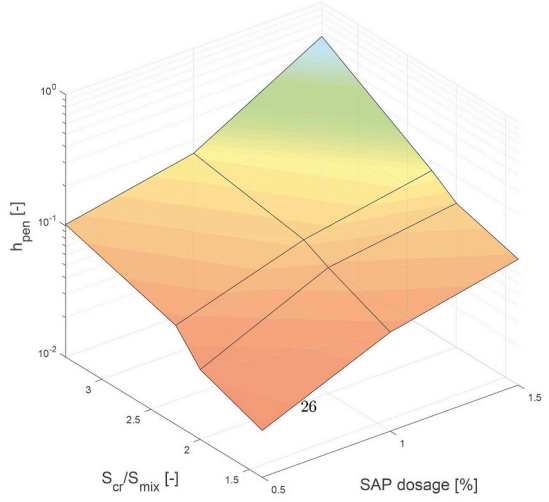

(b) $w_{cr} = 300\ \mu m$

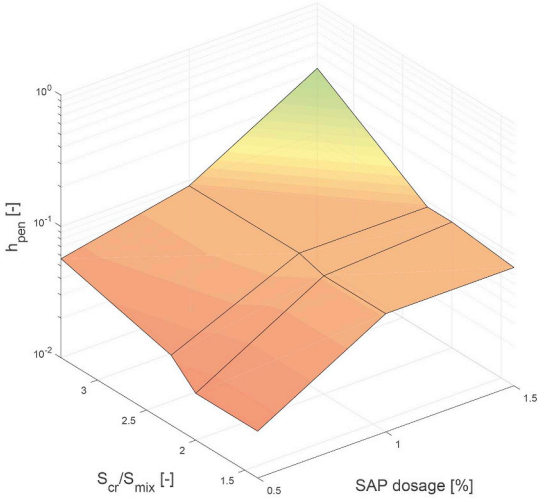

(c) $w_{cr} = 500\ \mu m$

Fig. 11. Parametric analysis of h_{pen} as a function of SAP dosage and swelling ratio for crack widths 200 μm a), 300 μm b) and 500 μm c).

By studying the surface plot corresponding to a crack width of 200 μm in 11a we can observe that for small values of the swelling ratio, such as the ones found for SAP B,1.37, increasing the dosage in the mortar from 0.5 $m\%$ to 1.5 $m\%$ does little to increase the self-sealing efficiency, resulting in an improvement from 4.5 % to only 10.2 %. On the other hand, for mortars containing as little as 0.5 $m\%$ of SAP, an increase on swelling ratio from 1.37 to 3.37 results in an improved self-sealing capacity that goes from 4.5 % to 21.6 %. This behavior seems to become less important as the crack width increases where the only combinations of dosage and swelling ratio yielding above 10 % sealing efficiency are those higher than 1.0 $m\%$ and 2.25, respectively. In general, within the chosen range of analyzed parameters, increasing the swelling ratio results in more efficient improvements on the swelling capacity than increasing the dosage within the suggested range. This observation implies that when choosing appropriate SAP for the purpose of crack self-sealing attention should be focused on the reduction of the absorption capacity during mixing as much as possible, that bulkly polymerized SAP are to be preferred to spherical ones because of the higher elastic properties and better deformation capacity and/or that the swelling capacity in neutral or acidic of the polymer be boosted. The capacity of swelling and absorption of SAP are properties which depend mainly on their composition and employed production method. Therefore their design can be steered for the purpose of self-sealing in cement-based materials according to what has been discussed in this section.

6. Conclusions

A numerical model is proposed in this work to simulate capillary water absorption in unsaturated sound and cracked cementitious materials with SAP. The results of the simulations yield the spatial moisture content distribution in the mortar during capillary absorption, as well as the water absorption of SAP in the matrix and in the crack and their swelling evolution. The model couples the Richards equation for liquid transport in porous media, the exponential equation describing the hydraulic diffusivity as a function of moisture content in porous building materials and the water absorption kinetics law for SAP particles modeled as sink terms. Lattice-type FEM was used to model the aforementioned mathematical problem. Distinction of transport properties was made explicitly between sound matrix, cracked domain and SAP particles. In the paper, the proposed model was validated first using experimental results and experimentally-informed input parameters available from literature or from experiments performed by the authors. The validated model was then used to investigate the influence of SAP absorption capacity and dosage in the mortar for different crack widths.

The following conclusions can be drawn from the comparison between experimental and simulated results and from the parametrical analysis performed herein:

1. If reswelling capacity of the SAP particles embedded in the matrix is considered completely recovered, SAP particles provoke two main anomalies in the moisture transport within a cementitious material i) the sorptivity of the composite increases because water uptake in the SAP occurs much faster than in the matrix and the polymer can absorb more water by unit volume than the plain mortar and ii) delays in the penetration depth of the wetting front are obtained due to the presence of almost impervious swollen gel, similar to the effect provoked by aggregates in concrete [49,50].
2. When reducing the nominal water absorption capacity of the SAP particles in the crack according to X-Ray tomography results, simulated results on capillary water absorption in cracked mortar with SAP matched very well the experimental ones. The poorer swelling capacity of the SAP in the crack can be explained more likely by the further cross linking and strong complexation in the polymer during mixing due to absorption of calcium ions [27,39]. In this regard current practices to estimate the necessary dosage of SAP, based on measured absorption capacity of SAP in the crack

must be modified i.e. by subjecting the polymers to cement filtrate absorption for a certain amount of time and only then to water absorption. Another cause of this deviation from measured free water swelling capacity of SAP can also be due to the constraint of the polymer between the crack walls.

3. The validation of the model with experimental results allowed us to look in detail at the effects of crack-self-sealing during capillary water absorption in cracked mortar via the simulations. There seems to be two main effects on the water transport from the cracks into the matrix: i) the penetration depth of the wetting front is delayed when hydrogel forms in the cracks and ii) moisture content distribution changes dramatically and zones with high degree of saturation are decreased. The later can be explained by the localized covering of the crack surface with hydrogel and the existence of moisture gradients along the crack walls and not only predominantly perpendicular to them.
4. The blockage of capillary rise in the crack only happens when there is a hydrogel plug occupying a cracked volume all across the specimen at a certain height, otherwise only the effects as described above are noticed. The occurrence of complete blockage of the capillary rise in the crack was, as expected, increased with increasing amount of SAP in the mixture and with a higher ratio of swelling capacity in the crack to swelling capacity during mixing.
5 When designing a cementitious mix with SAP, simulated results show that choosing appropriate SAP admixtures results in a more efficient crack self-sealing performance rather than increasing SAP dosage in the mix design. The choice of SAP to be used for crack self-sealing and (allegedly) self-healing, must be based upon increasing the swelling ratio. An option could be to limit the absorption and swelling of the polymer during mixing of the cement-based materials not only for the aforementioned reason but also to control the reduction of the mechanical properties. Nevertheless, this limit should not be accompanied by complexation in the polymer due to the intake of calcium ions not to affect the swelling of the particles in the incoming crack water. A second option would be to select SAP with higher swelling capacity in neutral to acidic media. In any case, bulkly polymerized SAP should be preferred to spherical ones.

We expect that this model can serve also as a basis for the modelling of mineral precipitation in the cracks of cementitious materials with SAP by coupling the sink/source behaviour of SAP particles proposed in this study into a multi-species reactive transport model.

Conflicts of interest

Declaration of interest

None.

Acknowledgements

C. Romero Rodriguez acknowledges the financial support from the Construction Technology Research Program funded by the Ministry of Land, Infrastructure and Transport of the Korean Government under the grant 17SCIP-B103706-03 and also the financial aid of the Cost Action 15202 under the Short Scientific Mission reference number 39002, in the realisation of the experiments. S. Chaves Figueiredo would like to acknowledge the funding from Science Without Borders from the National Council for Scientific and Technological Development of Brazil (201620/2014-6).

References

[1] H. Lee, H. Wong, N. Buenfeld, Potential of superabsorbent polymer for self-sealing cracks in concrete, Adv. Appl. Ceram. 109 (5). doi:10.1179/174367609X459559. URL http://www.tandfonline.com/doi/full/10.1179/174367609X459559.

[2] A. Katchalsky, I. Michaeli, Polyelectrolyte gels in salt solutions, J. Polym. Sci. 15 (79) (1955) 69–86, https://doi.org/10.1002/pol.1955.120157906.

[3] S. Vervoort, Behaviour of Hydrogels Swollen in Polymer Solutions under Mechanical Action, Phd Dissertation, Ecole Nationale Superieure des Mines de Paris, 2006.

[4] O.M. Jensen, P.F. Hansen, Water-entrained cement-based materials: ii. experimental observations, Cement Concr. Res. 32 (6) (2002) 973–978.

[5] V. Mechtcherine, C. Schröfl, M. Wyrzykowski, M. Gorges, P. Lura, D. Cusson, J. Margeson, N. De Belie, D. Snoeck, K. Ichimiya, S.-I. Igarashi, V. Falikman, S. Friedrich, J. Bokern, P. Kara, A. Marciniak, H.-W. Reinhardt, S. Sippel, A. Bettencourt Ribeiro, J. Custódio, G. Ye, H. Dong, J. Weiss, Effect of superabsorbent polymers (SAP) on the freeze–thaw resistance of concrete: results of a RILEM interlaboratory study, Mater. Struct. 50 (1). doi:10.1617/s11527-016-0868-7. URL http://link.springer.com/10.1617/s11527-016-0868-7.

[6] J.S. Kim, E. Schlangen, Super absorbent polymers to stimulate self healing in ECC, 2nd International Symposium on Service Life Design for Infrastructure, No. 1, 2010, pp. 849–858.

[7] D. Snoeck, K. Van Tittelboom, S. Steuperaert, P. Dubruel, N. De Belie, Self-healing cementitious materials by the combination of microfibres and superabsorbent polymers, J. Intell. Mater. Syst. Struct. 25 (1) (2014) 13–24.

[8] B. Craeye, M. Geirnaert, G. De Schutter, Super absorbing polymers as an internal curing agent for mitigation of early-age cracking of high-performance concrete bridge decks, Constr. Build. Mater. 25 (1) (2011) 1–13.

[9] J. Justs, M. Wyrzykowski, D. Bajare, P. Lura, Internal curing by superabsorbent polymers in ultra-high performance concrete, Cement Concr. Res. 76 (2015) 82–90.

[10] S. Laustsen, M.T. Hasholt, O.M. Jensen, Void structure of concrete with superabsorbent polymers and its relation to frost resistance of concrete, Mater. Struct. 48 (1–2) (2015) 357–368.

[11] S. Mönnig, P. Lura, Superabsorbent polymers—an additive to increase the freeze-thaw resistance of high strength concrete, Advances in Construction Materials 2007, Springer, 2007, pp. 351–358.

[12] H. Lee, H. Wong, N. Buenfeld, Self-sealing of cracks in concrete using superabsorbent polymers, Cement Concr. Res. 79 (2016) 194–208, https://doi.org/10.1016/j.cemconres.2015.09.008 http://linkinghub.elsevier.com/retrieve/pii/S0008884615002458.

[13] G. Hong, S. Choi, Rapid self-sealing of cracks in cementitious materials incorporating superabsorbent polymers, Constr. Build. Mater. 143 (2017) 366–375, https://doi.org/10.1016/j.conbuildmat.2017.03.133 http://linkinghub.elsevier.com/retrieve/pii/S0950061817305202.

[14] D. Snoeck, S. Steuperaert, K. Van Tittelboom, P. Dubruel, N. De Belie, Visualization of water penetration in cementitious materials with superabsorbent polymers by means of neutron radiography, Cement Concr. Res. 42 (8) (2012) 1113–1121, https://doi.org/10.1016/j.cemconres.2012.05.005 https://doi.org/10.1016/j.cemconres.2012.05.005.

[15] G. Hong, S. Choi, Modeling rapid self-sealing of cracks in cementitious materials using superabsorbent polymers, Constr. Build. Mater. 164 (2018) 570–578, https://doi.org/10.1016/j.conbuildmat.2018.01.017 http://linkinghub.elsevier.com/retrieve/pii/S0950061818300175.

[16] L.A. Richards, Capillary conduction of liquids through porous mediums, Physics 1 (5) (1931) 318–333.

[17] A. Szymkiewicz, Modelling Water Flow in Unsaturated Porous Media vol. 9, Springer, 2013, https://doi.org/10.1007/978-3-642-23559-7 http://link.springer.com/10.1007/978-3-642-23559-7.

[18] C. Hall, W.D. Hoff, second ed., Water Transport in Brick, Stone and Concrete vol. 25, Spon Press, 2009, https://doi.org/10.1520/CCA10518J.

[19] D. Lockington, J.-Y. Parlange, P. Dux, Sorptivity and the estimation of water penetration into unsaturated concrete, Mater. Struct. 32 (5) (1999) 342.

[20] B. Šavija, M. Luković, E. Schlangen, Influence of cracking on moisture uptake in strain-hardening cementitious composites, J. Nanomech. Micromech. 7 (1) (2017) 04016010, , https://doi.org/10.1061/(ASCE)NM.2153-5477.0000114 http://ascelibrary.org/doi/10.1061/%28ASCE%29NM.2153-5477.0000114.

[21] L. Wang, J. Bao, T. Ueda, Prediction of mass transport in cracked-unsaturated concrete by mesoscale lattice, Ocean. Eng. 127 (2016) 144–157, https://doi.org/10.1016/j.oceaneng.2016.09.044 August https://doi.org/10.1016/j.oceaneng.2016.09.044.

[22] Y. Mualem, A new model for predicting the hydraulic conductivity of unsaturated porous media, Water Resour. Res. 12 (3) (1976) 513–522.

[23] M.T. Van Genuchten, A closed-form equation for predicting the hydraulic conductivity of unsaturated soils 1, Soil Sci. Soc. Am. J. 44 (5) (1980) 892–898.

[24] L.P. Esteves, Superabsorbent polymers: on their interaction with water and pore fluid, Cement Concr. Compos. 33 (7) (2011) 717–724, https://doi.org/10.1016/j.cemconcomp.2011.04.006.

[25] T. Sweijen, C. van Duijn, S. Hassanizadeh, A model for diffusion of water into a swelling particle with a free boundary: application to a super absorbent polymer particle, Chem. Eng. Sci. 172 (2017) 407–413, https://doi.org/10.1016/j.ces.2017.06.045 https://doi.org/10.1016/j.ces.2017.06.045.

[26] C. Schröfl, D. Snoeck, V. Mechtcherine, A review of characterisation methods for superabsorbent polymer (SAP) samples to be used in cement-based construction materials: report of the RILEM TC 260-RSC, Mater. Struct. 50 (4). doi:10.1617/s11527-017-1060-4. URL http://link.springer.com/10.1617/s11527-017-1060-4.

[27] H. Lee, H. Wong, N. Buenfeld, Effect of alkalinity and calcium concentration of pore solution on the swelling and ionic exchange of superabsorbent polymers in cement paste, Cement Concr. Compos. 88 (2018) 150–164, https://doi.org/10.1016/j.cemconcomp.2018.02.005 http://linkinghub.elsevier.com/retrieve/pii/S0958946518301483.

[28] E. Schlangen, J.G.M. van Mier, Experimental and numerical analysis of

micromechanisms of fracture of cement-based composites, Cement Concr. Compos. (14) (1992) 105–118.
[29] B. Šavija, J. Pacheco, E. Schlangen, Lattice modeling of chloride diffusion in sound and cracked concrete, Cement Concr. Compos. 42 (2013) 30–40, https://doi.org/10.1016/j.cemconcomp.2013.05.003.
[30] P. Grassl, J. Bolander, Three-dimensional network model for coupling of fracture and mass transport in quasi-brittle geomaterials, Materials 9 (9) (2016) 1–18, https://doi.org/10.3390/ma9090782 arXiv:1510.05184.
[31] Z. Qian, E. Garboczi, G. Ye, E. Schlangen, Anm: a geometrical model for the composite structure of mortar and concrete using real-shape particles, Mater. Struct. 49 (1–2) (2016) 149–158.
[32] N. Nestle, A. Kühn, K. Friedemann, C. Horch, F. Stallmach, G. Herth, Water balance and pore structure development in cementitious materials in internal curing with modified superabsorbent polymer studied by nmr, Microporous Mesoporous Mater. 125 (1–2) (2009) 51–57.
[33] D. Asahina, K. Kim, Z. Li, J.E. Bolander, Flow field calculations within discrete models of multiphase materials, Compos. B Eng. 58 (2014) 293–302, https://doi.org/10.1016/j.compositesb.2013.10.043 https://doi.org/10.1016/j.compositesb.2013.10.043.
[34] M. Luković, B. Šavija, E. Schlangen, G. Ye, K. van Breugel, A 3D lattice modelling study of drying shrinkage damage in concrete repair systems, Materials 9 (7). doi:10.3390/MA9070575.
[35] D. Snoeck, Self-Healing and Microstructure of Cementitious Materials with Microfibres and Superabsorbent Polymers, Phd dissertation Ghent University, 2015.
[36] D. Snoeck, L. Velasco, A. Mignon, S. Van Vlierberghe, P. Dubruel, P. Lodewyckx, N. De Belie, The effects of superabsorbent polymers on the microstructure of cementitious materials studied by means of sorption experiments, Cement Concr. Res. 77 (2015) 26–35, https://doi.org/10.1016/j.cemconres.2015.06.013 http://linkinghub.elsevier.com/retrieve/pii/S0008884615001829.
[37] J. Philip, The theory of infiltration: 5. the influence of the initial moisture content, Soil Sci. 84 (4) (1957) 329–340.
[38] W. Brutsaert, The concise formulation of diffusive sorption of water in a dry soil, Water Resour. Res. 12 (6) (1976) 1118–1124.
[39] D. Snoeck, L.F. Velasco, A. Mignon, S. Van Vlierberghe, P. Dubruel, P. Lodewyckx, N. De Belie, The effects of superabsorbent polymers on the microstructure of cementitious materials studied by means of sorption experiments, Cement Concr. Res. 77 (2015) 26–35, https://doi.org/10.1016/j.cemconres.2015.06.013 https://doi.org/10.1016/j.cemconres.2015.06.013.
[40] D. Snoeck, Zelfhelend Beton Door Combinatie Van Microvezels Met Reactieve Stoffen, Master's thesis Universiteit Gent, Ghent, 2011.
[41] C. Romero Rodriguez, S. Chaves Figueiredo, D. Snoeck, B. Šavija, E. Schlangen, Modelling strategies for the study of crack self-sealing in mortar with superabsorbent polymers, in: E. Schlangen, G. de Schutter, B. Šavija, H. Zhang, C. Romero Rodriguez (Eds.), Proceedings of the Symposium on Concrete Modelling, Vol. PRO 127 of Rilem Proceedings, Rilem, 2018, pp. 333–341 green Open Access added to TU Delft Institutional Repository 'You share, we take care!' – Taverne project https://www.openaccess.nl/en/you-share-we-take-care Otherwise as indicated in the copyright section: the publisher is the copyright holder of this work and the author uses the Dutch legislation to make this work public).
[42] B. Masschaele, M. Dierick, D. Van Loo, M.N. Boone, L. Brabant, E. Pauwels, V. Cnudde, L. Van Hoorebeke, Hector: a 240kv micro-ct setup optimized for research, Journal of Physics: Conference Series, vol. 463, IOP Publishing, 2013012012.
[43] I. Arganda-Carreras, V. Kaynig, C. Rueden, K.W. Eliceiri, J. Schindelin, A. Cardona, H. Sebastian Seung, Trainable weka segmentation: a machine learning tool for microscopy pixel classification, Bioinformatics 33 (15) (2017) 2424–2426, https://doi.org/10.1093/bioinformatics/btx180 arXiv:/oup/backfile/content_public/journal/bioinformatics/33/15/10.1093_bioinformatics_btx180/3/btx180.pdf https://doi.org/10.1093/bioinformatics/btx180.
[44] H.W. Reinhardt, A. Assmann, Enhanced durability of concrete by superabsorbent polymers, Proc. BMC, vol. 9, 2009, pp. 291–300.
[45] H. Wong, A. Pappas, R. Zimmerman, N. Buenfeld, Effect of entrained air voids on the microstructure and mass transport properties of concrete, Cement Concr. Res. 41 (10) (2011) 1067–1077, https://doi.org/10.1016/j.cemconres.2011.06.013 http://linkinghub.elsevier.com/retrieve/pii/S0008884611001876.
[46] D. Liu, B. Šavija, G.E. Smith, P.E.J. Flewitt, T. Lowe, E. Schlangen, Towards understanding the influence of porosity on mechanical and fracture behaviour of quasi-brittle materials: experiments and modelling, Int. J. Fract. 205 (1) (2017) 57–72, https://doi.org/10.1007/s10704-017-0181-7 http://link.springer.com/10.1007/s10704-017-0181-7.
[47] Y. Yao, Y. Zhu, Y. Yang, Incorporation superabsorbent polymer (sap) particles as controlling pre-existing flaws to improve the performance of engineered cementitious composites (ecc), Constr. Build. Mater. 28 (1) (2012) 139–145.
[48] D. Snoeck, T. De Schryver, N. De Belie, Enhanced impact energy absorption in self-healing strain-hardening cementitious materials with superabsorbent polymers, Constr. Build. Mater. 191 (2018) 13–22.
[49] C.R. Rodríguez, S.C. Figueiredo, E. Schlangen, D. Snoeck, Modeling water absorption in cement-based composites with sap additions, Computational Modelling of Concrete Structures: Proceedings of the Conference on Computational Modelling of Concrete and Concrete Structures (EURO-C 2018), February 26-March 1, 2018, Bad Hofgastein, CRC Press, Austria, 2018, p. 295.
[50] X. Li, S. Chen, Q. Xu, Y. Xu, Modeling the three-dimensional unsaturated water transport in concrete at the mesoscale, Comput. Struct. 190 (2017) 61–74, https://doi.org/10.1016/j.compstruc.2017.05.005 http://linkinghub.elsevier.com/retrieve/pii/S0045794917302766.
[51] D. Gardner, A. Jefferson, A. Hoffman, Investigation of capillary flow in discrete cracks in cementitious materials, Cement Concr. Res. 42 (7) (2012) 972–981, https://doi.org/10.1016/j.cemconres.2012.03.017 http://linkinghub.elsevier.com/retrieve/pii/S0008884612000701.